LBL-1476

EVALUATION OF THE END QUENCH TEST AS A DESIGN CRITERION

Roy Neal Lott
(M.S. thesis)

June 1973

Prepared for the U.S. Atomic Energy Commission
under Contract W-7405-ENG-48

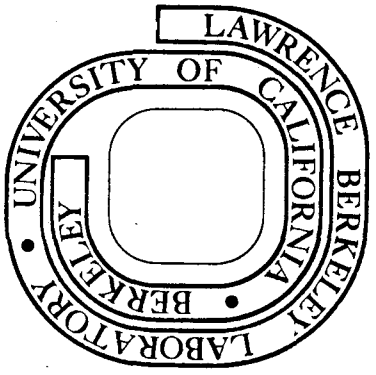

LBL-1476

DISCLAIMER

TABLE OF CONTENTS

EVALUATION OF THE END QUENCH TEST AS A DESIGN CRITERION

Roy Neal Lott

Inorganic Materials Research Division, Lawrence Berkeley Laboratory and Department of Materials Science and Engineering, College of Engineering; University of California, Berkeley, California

ABSTRACT

End quench test results have commonly been used to design quenching conditions in the hope that the desired microstructure will be obtained in the quenched piece. Investigation of this practice shows it to be invalid in principle. The correlation of end quench data to other quenching conditions is based either on equivalent measured final hardness values or, more generally, on equivalent cooling rates at 1300°F during quenching. The correlation based on equivalent hardness values is invalid because hardness is not a sensitive indication of microstructure or properties of a quenched steel. Correlations based on equivalent cooling rates are not valid because the final properties are shown not to be dependent on the cooling rate at 1300°F during the quench. This is because the final microstructure of a quenched piece depends on the path of the cooling curve through the continuous cooling transformation diagram. The shape of the cooling curve is a function of the quenching conditions and, therefore, its path is not determined by the cooling rate at 1300°F.

I. INTRODUCTION

It is common in the literature to find descriptions of the end quench test which indicate that the microstructure, and therefore the properties, of a quenched piece of steel can be predicted from cooling rate data and the hardenability curve for a steel. For example, U.S. Steel states: "This test [the end quench test] furnishes a method of applying a continuous series of varying cooling rates to a single specimen, and, since these rates are known, the results can be converted to hardenability values in terms of ideal diameter. The curve used for this conversion is shown in Figure 40-38 (See Fig. 1). To use this curve, the distance along the end quench bar to the desired microstructure, or corresponding hardness value, is noted and the ideal diameter corresponding to this distance is read from the curve. This ideal diameter may then be converted into terms of bar size which can be hardened under any given quenching conditions ..."[1] With regard to conversion from ideal diameter to bar size, this source also states: "Since the cooling rate relationships between the ideal quench and other quenching conditions are known, hardenability values in terms of ideal diameter can be used to predict the size of round which will harden in any quench ..."[1] The ideal diameter--size of round correlations are illustrated in Fig. 2. Van Vlack says: "End quench hardenability curves are of great practical value because (1) if the cooling rate of a steel in any quench is known, the hardness may be read directly from the hardenability curve for that steel, and (2) if the hardness at any point can be measured, the cooling rate at that

Fig. 1.

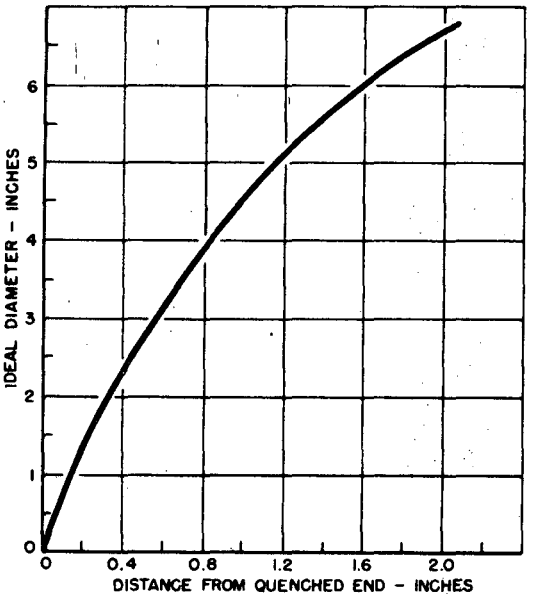

FIG. 40—38. Curve for converting distance from quenched end corresponding to the desired microstructure (or hardness) in the end-quench test to hardenability values in terms of ideal diameter. (After Carney)

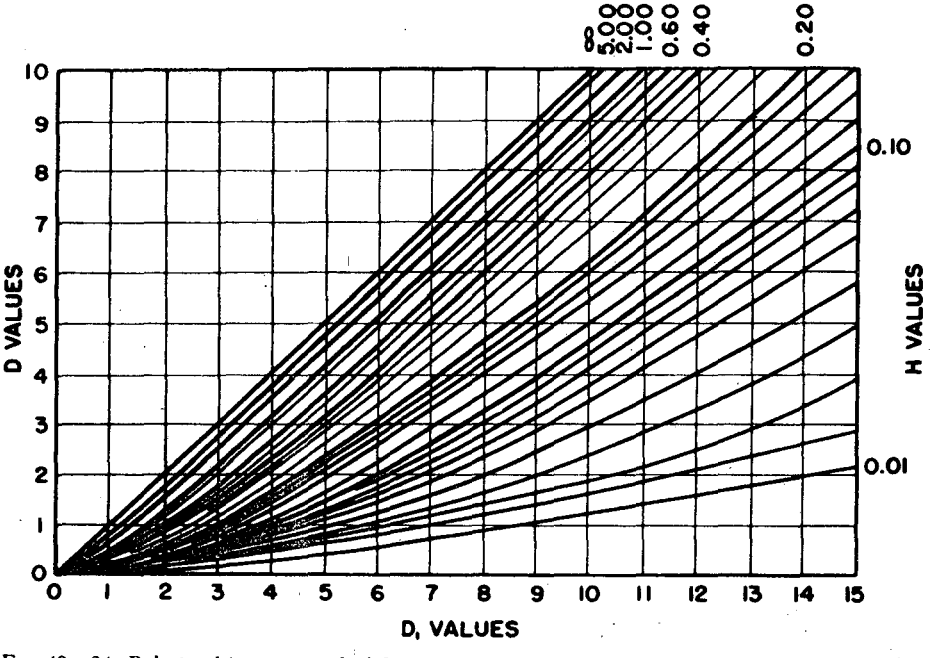

FIG. 40—34. Relationships among ideal diameter, critical diameter and severity of quench.

XBL 735-581

Fig. 2. Example figures, as found in literature, relating end quench data to the designing of quenching conditions. (From U.S. Steel[1])

A. S. T. M. END QUENCH TEST FOR HARDENABILITY OF STEEL A 255

DATE_____
LABORATORY_____
TYPE SPECIMEN_____
TEST NO._____

TYPE	HEAT NO.	GRAIN SIZE	C	Mn	P	S	Si	Ni	Cr	Mo		NORM. TEMP. °F.	QUENCH TEMP. °F.
8740	19297	8-7	.44	.89	.019	.016	.27	.58	.50	.25		1650	1550
8620	621271	7-8	.19	.80	.015	.015	.23	.46	.52	.22		1700	1700

REMARKS:

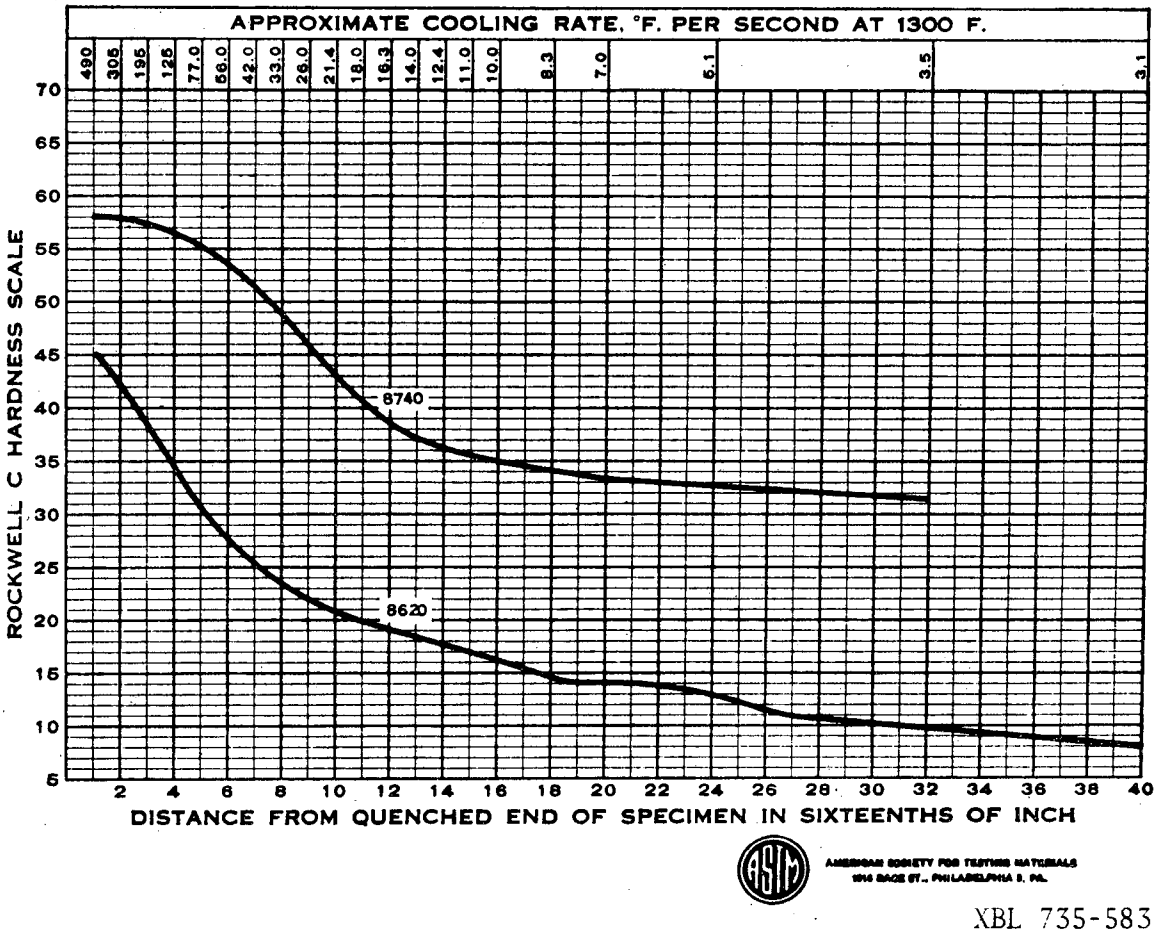

Fig. 3. Typical hardenability curves with related end quench cooling rates at 1300°F. (ASTM Standards[5])

point may be obtained from the hardenability curve (See Fig. 3) for that steel."[2]

As shown in Fig. 3, the hardenability curve is based on the cooling rate at 1300°F, which would be in the pearlite region in most continuous cooling transformation diagrams. It is the contention of this thesis that, in general, the microstructure of a quenched piece of steel cannot be accurately predicted from the cooling rate at 1300°F (or any other temperature). For a given steel, it may be possible to determine a temperature from an accurate continuous cooling transformation diagram at which the cooling rate can be directly related to the final microstructure. However, no single temperature applies for all steels. The cooling rate at 1300°F relationships, which are conventionally used to predict quenched microstructure, are invalid because the path of the cooling curve through the continuous cooling transformation diagram cannot be predicted from the cooling rate at 1300°F. That is, two quench pieces of different sizes or geometries, and quenched in different media, may have identical cooling rates at 1300°F, but their cooling curves may follow different paths at lower temperatures, as illustrated in Fig. 4. The types and amounts of bainite and martensite formed during transformation at the lower temperatures will greatly affect the final properties of the quench piece.[3] Variations of the cooling curve through the bainite-martensite regions can produce wide variations in mechanical properties.

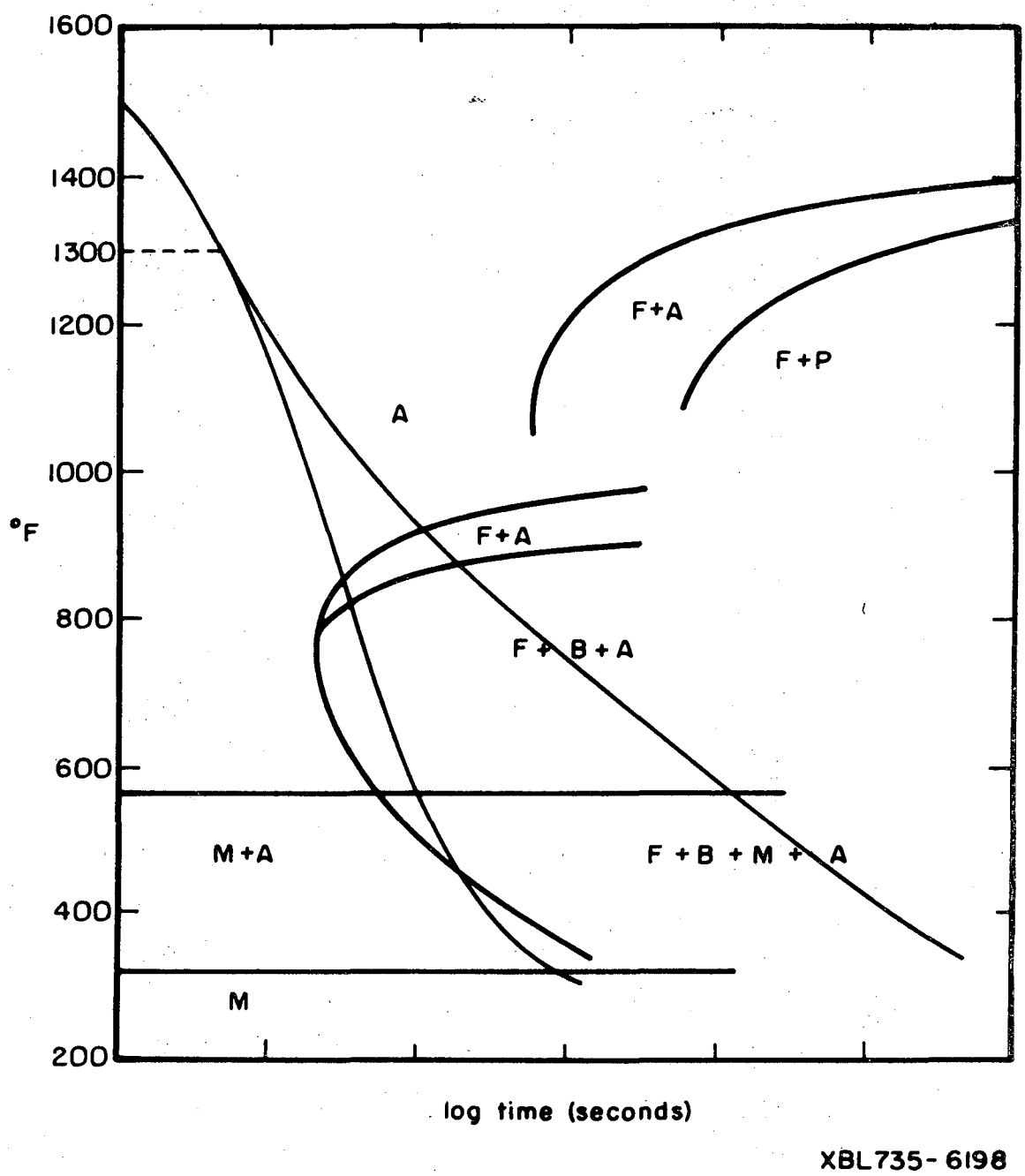

Fig. 4. Two cooling curves that have equal cooling rates at 1300°F but take different paths through the continuous cooling transformation diagram due to differences in quenching conditions.

Some of the ideal diameter--round size correlations are based on hardness measurements using the theory that points of equal hardness had equal cooling rates and vice versa. However, the hardness--cooling rate at 1300°F correlation is not an exact one and, also, hardness is not a good indication of the other properties of a piece of steel. The hardness may show a good correlation to strength but it gives no indication of toughness or ductility.[4] The properties of two pieces with identical center hardnesses may be quite different thus making quenching condition correlations based on hardness measurements as invalid as those based on cooling rates at 1300°F.

The purpose of this experimentation was to demonstrate that quenching correlations based on the end quench test or the ideal diameter concept are not necessarily accurate. Diagrams such as Figs. 1, 2, and 3 are, of course, useful in many instances, but users should be aware of their limitations.

II. EXPERIMENT DESCRIPTIONS

A. The End Quench Experiment

In order to show that properties of a quenched piece cannot be accurately predicted from end quench data, a modified end quench specimen was designed so that the Charpy V-notch impact toughness property could be measured along its length. The end quench specimen, which is shown in Fig. 5, was redesigned to have a rectangular cross-section so that it could be cut into Charpy V-notch bars after heat treatment. The modified end quench specimen was roughly comparable to the standard Jominy bar[5] in that it had a similar quench end face area (0.854 $in.^2$ vs 0.785 $in.^2$ standard) and length (4.125 in. vs 4.00 in. standard).

The end quenching rig was also modified with a rectangular nozzle and orifice to accommodate the rectangular end quench specimen as shown in Fig. 6. All other aspects of the end quench treatment were done in accord with the ASTM Standard Method of End Quench Test for Hardenability of Steels, A255-67.[5] The ratio of orifice area/quench end face area was 1/4. A free height of $2\frac{1}{2}$ in. above the orifice was maintained by the vertical stream of water which was gravity fed from a constant surface level reservior to the nozzle. The nozzle was designed such that a fairly uniform velocity was maintained over the cross-section of the vertical stream of water. The bottom end face of the end quench specimen supported $\frac{1}{2}$ in. above the nozzle orifice. The modified end quench specimen compared closely with the standard

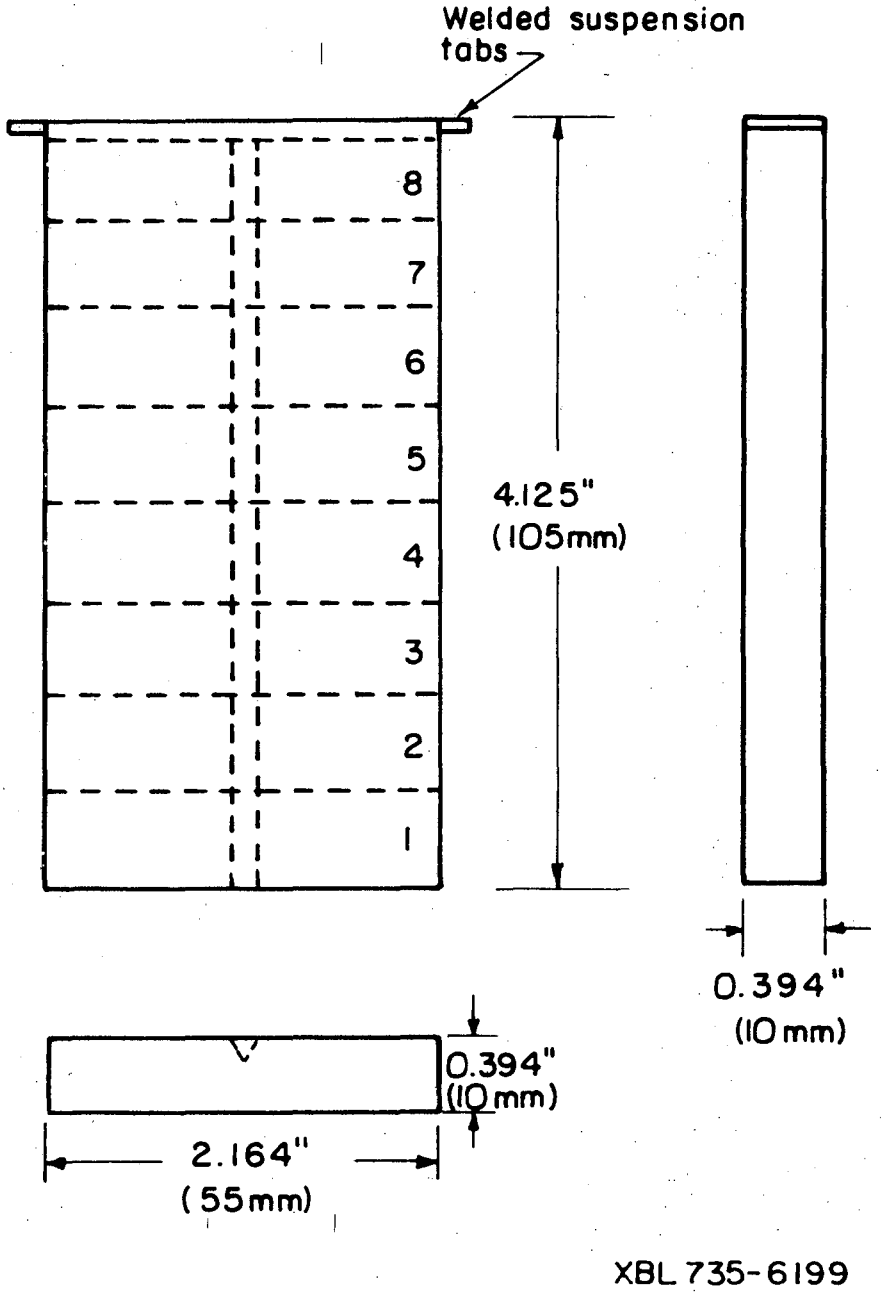

Fig. 5. The modified end quench specimen; dotted lines indicate where the specimen was subsequently V-notched and cut into Charpy bars. The hardness tests were made along the notch line prior to cutting the notch.

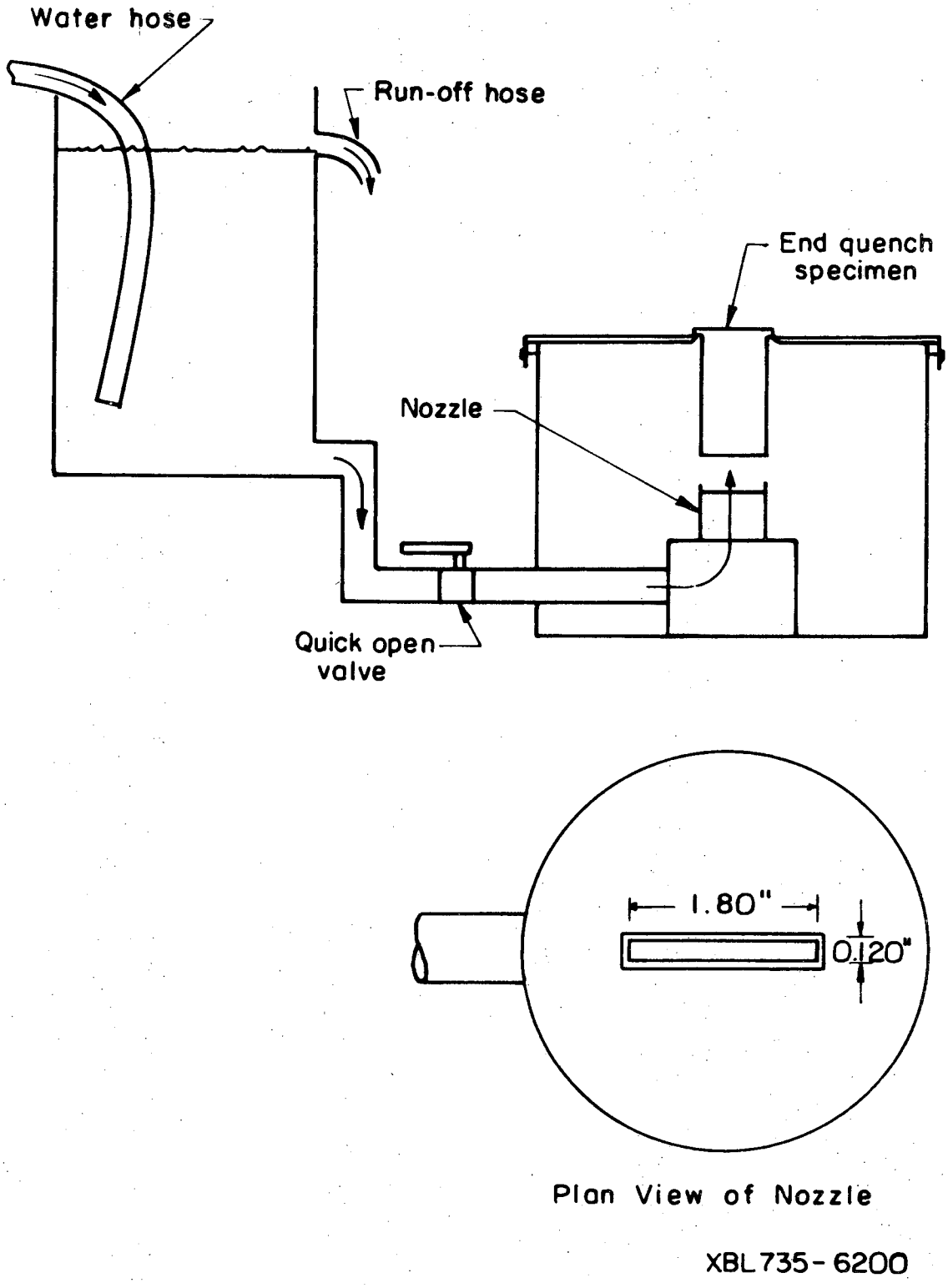

Fig. 6. The End Quenching Rig.

on the basis of cooling rates at 1300°F and hardness curves. (These details will be discussed in the "Experimental Procedure and Results" section.) After the end quench heat treatment and machining of the end quench specimens into Charpy bars, brittle transition temperature curves and tempering curves were obtained for each Charpy bar position on the end quench specimen in order to describe the toughness behavior along the end quench specimen.

B. The Bundle Quench Experiment

Charpy bars of the same steel as the end quench specimens were individually bound in the center of a bundle of steel blocks (as shown in Fig. 7) and heat treated. The cooling curves of the bundled Charpy bars were recorded during quenching of the bundles in both agitated oil and agitated water. On the basis of the cooling rate at 1300°F, the toughness properties of the bundle quenched bars were compared to those predicted by the end quench data. The toughness behavior of the bundle quenched bars differed significantly from that predicted from the end quench data. Also, the hardness values measured at the center of the bundle quenched Charpy bars after fracture were compared to those from the end quench hardenability curves for the same cooling rates. The hardness values of the bundle quench bars did not correspond accurately to the hardenability curves for the same cooling rates, contrary to the previously quoted statement from Van Vlack.[2] These results show that the end quench test does not necessarily provide an accurate means for predicting the properties of a quenched piece of steel.

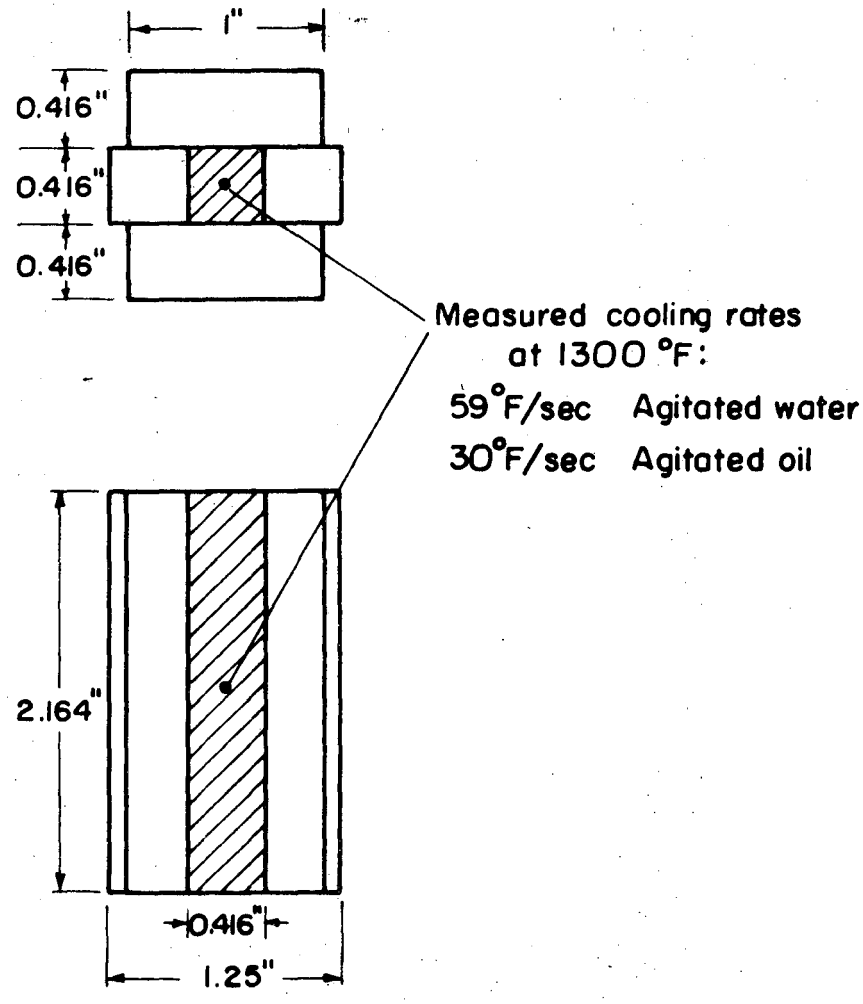

Fig. 7. The bundle quenched bar; a Charpy bar bound in a bundle of steel blocks.

C. The Bar Section Quench Experiment

In order to illustrate the effect of specimen size and geometry, and of the quenching medium, on the shape of the cooling curve, the cooling curves of round bar sections of various sizes were recorded during quenching in agitated oil and agitated water. Thermocouples were placed at bar centers and bar half radii in cylinders 1, $1\frac{1}{2}$, 2, $2\frac{1}{2}$, and 3 inches in diameter. For each bar center and half radius the cooling rate at 1300°F was plotted against the cooling rate at 700°F for agitated oil and agitated water quenches. This plot (Fig. 14) clearly shows that two quenched pieces with the same cooling rate at 1300°F can differ greatly in cooling rate at a lower temperature (700°F in this case). The shapes of cooling curves vary significantly with variations in quenching conditions.

III. EXPERIMENTAL PROCEDURE AND RESULTS

A. The End Quench

The end quench and bundle quench impact toughness experiments were performed using the following steels:

S.A.E. No.	C	Mn	P	S	Si	Cr	Ni	Mo	Cu	E.H.N. Gr. Size	Condition
4130	.29	.51	.015	.015	.26	.96	.12	.20	.15	5/8	Normalized
4340	.41	.85	.015	.016	.32	.82	1.78	.25	.16	5/8	Annealed

Both alloys were ladle vacuum degassed, aircraft grade steels. The modified end quench specimens were machined to 0.394 in. (10 mm) × 2.164 in. (55 mm) × 4.125 in. (105 mm) dimensions with the rolling direction of the steel parallel to the length of the specimen. Support tabs were welded on the end of each specimen.

Thermocouple tips were implanted at the specimen mid-thickness at various distances from the quenched end; the cooling curves were recorded during end quenching. The cooling rates at 1300°F were determined from the recorded cooling curves and were compared with the published cooling rate curves for standard Jominy end quench specimens. It was found that the cooling rate curve from the modified end quench specimen compared closely to the standard (as shown in Fig. 8). After heat treatment the specimens were hand sanded and Rockwell C hardness tests were made along the lengths of the specimens in order to determine how closely the modified specimen hardenability curves reproduced

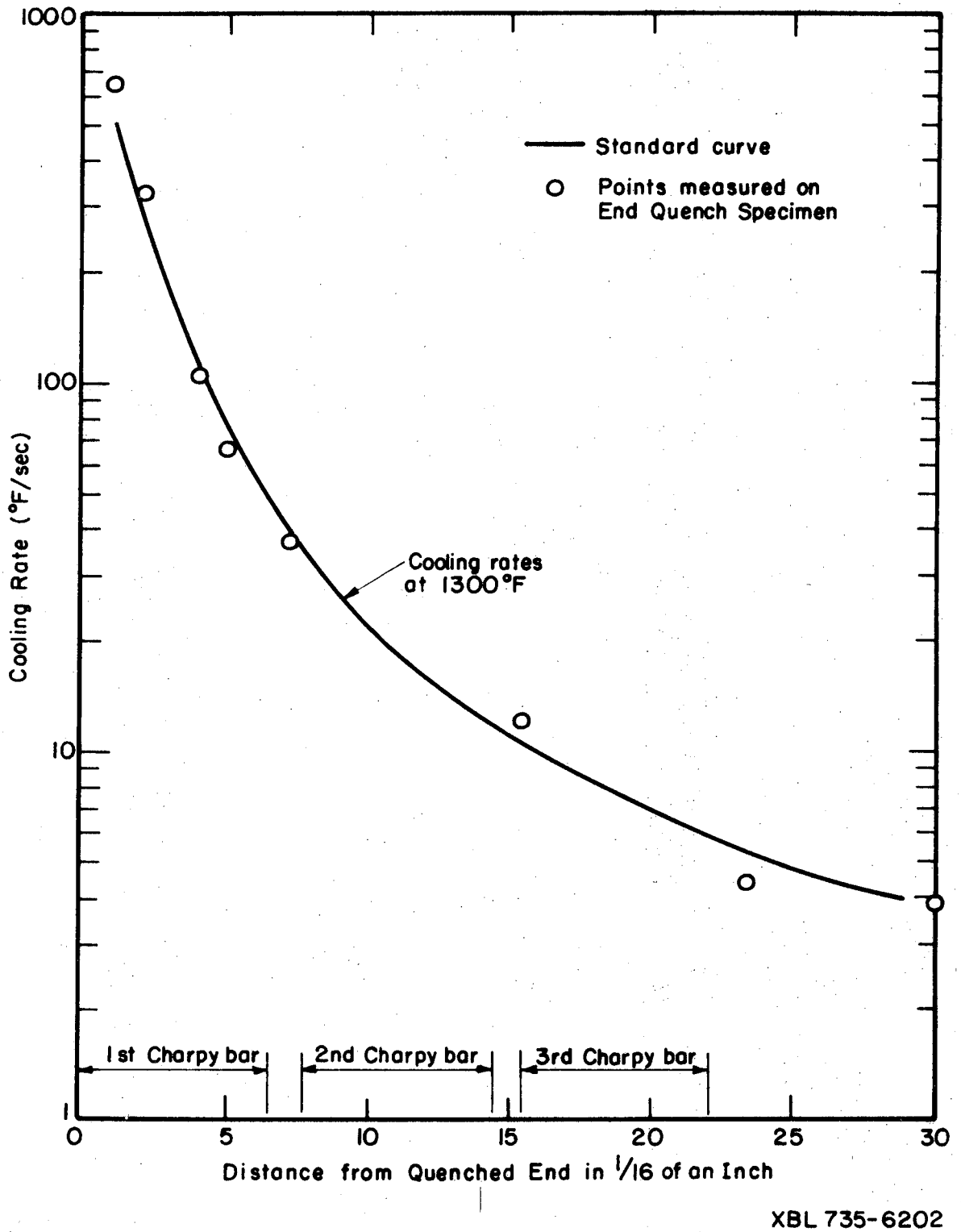

Fig. 8. Comparison of cooling rates at 1300°F measured along the modified end quench specimen to the published cooling rate curve for the standard end quench test.

published hardenability curve limits for 4130 and 4340 steels. The average hardness values measured along the length of the end quench specimens are given in Table 1. The modified specimen end quench was found to be closely comparable to the standard end quench test by the criteria of cooling rates at 1300°F and hardenability curves.

Two different heat treatments were used in this experiment; the standard end quench test and a two step heat treatment. William E. Wood found that by heating to 2200°F and then cooling relatively slowly to the standard austenitizing temperature (1550°F for 4340, 1600°F for 4130 steel) before quenching in oil or water caused the fracture toughness of these alloys to be greatly improved.[3] In order to supplement the investigation of the austenitizing temperature effect, some of the specimens were given this two stage step quench heat treatment prior to end quenching. The standard end quench heat treatment consisted of placing the specimen in a furnace at the standard austenitizing temperature for 30 min. then quickly transferring the specimen to the quenching rig where the bottom end of the specimen was spray quenched for 10 min. with water 68 to 70°F in temperature. The specimen was immersed in water immediately after the 10 min. end quench. The step quench heat treatment was exactly like the standard treatment except the specimen was placed in a furnace at 2200°F for 1 hr. before being transferred to the furnace at standard austenitizing temperature, where it was held until it reached temperature uniformity at the lower temperature. All furnaces used for these heat treatments

Table 1. The Average Hardenability Curves for End Quench Specimens Given the Standard Heat Treatment.

Average R_c Hardness Values Along the Seven Specimens of Each Alloy Given the Standard End Quench		
Distance (inches)	4130 Alloy	4340 Alloy
1/16	50.5	56.2
2/16	50.2	55.7
3/16	48.4	55.3
4/16	45.0	55.0
5/16	41.6	54.7
6/16	38.6	54.6
7/16	36.3	54.3
8/16	34.2	54.3
9/16	32.7	54.2
10/16	31.6	54.1
11/16	30.4	53.8
12/16	30.0	53.6
13/16	29.3	53.5
14/16	28.6	53.2
15/16	28.7	53.1
1	27.7	52.9
1 1/4	26.3	52.2
1 1/2	25.7	51.6
1 3/4	25.0	51.0
2	23.4	49.9
2 1/4	22.6	48.5
2 1/4	21.5	47.4
2 3/4	19.6	46.6
3	19.2	45.1
3 1/4	17.4	44.4
3 1/2	18.1	44.0
3 3/4	18.3	43.9
4	16.2	43.5

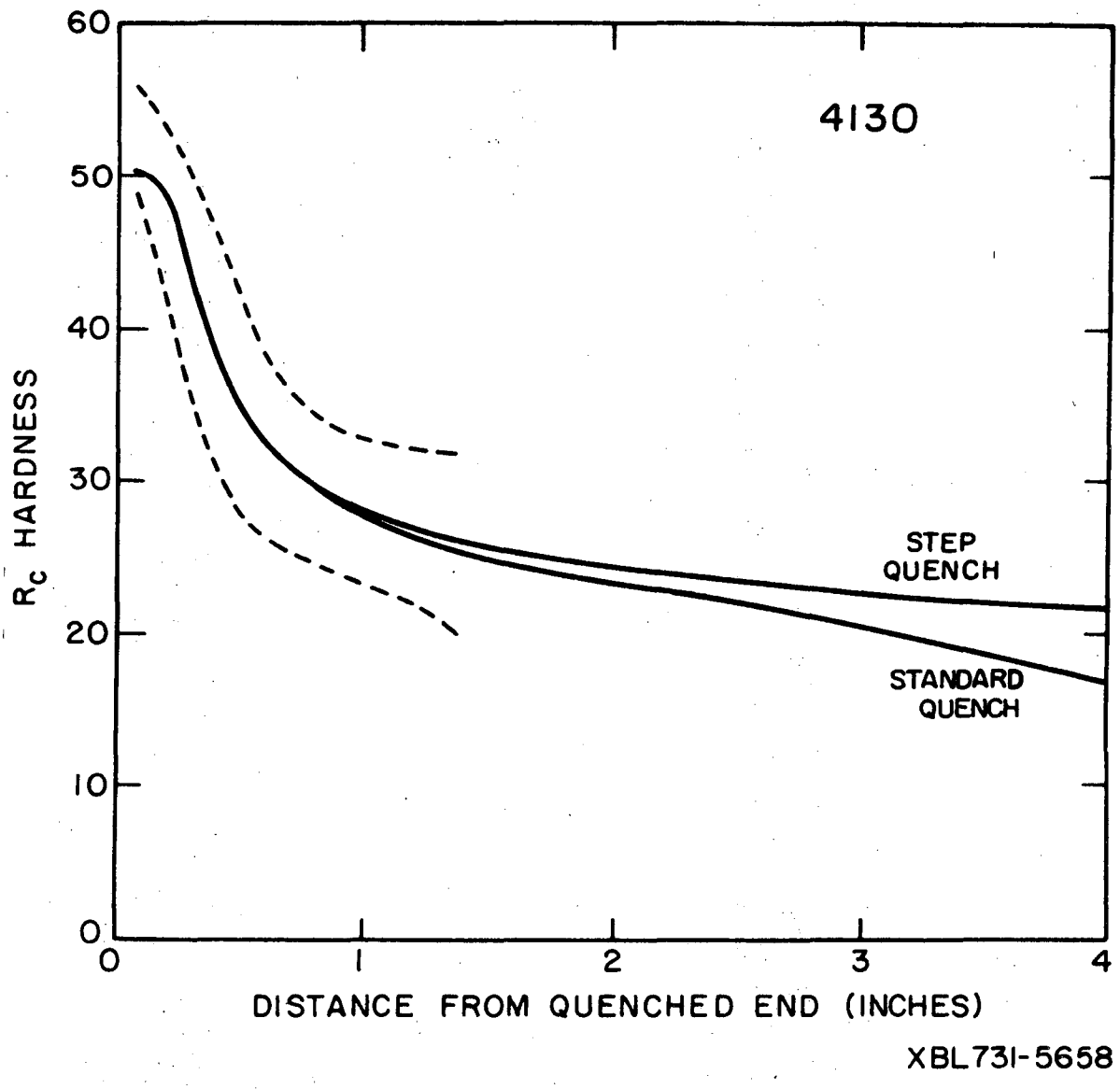

Fig. 9. The average hardenability curves for the 4130 steel end quench specimens. The dotted lines represent published hardenability curve limits.[8]

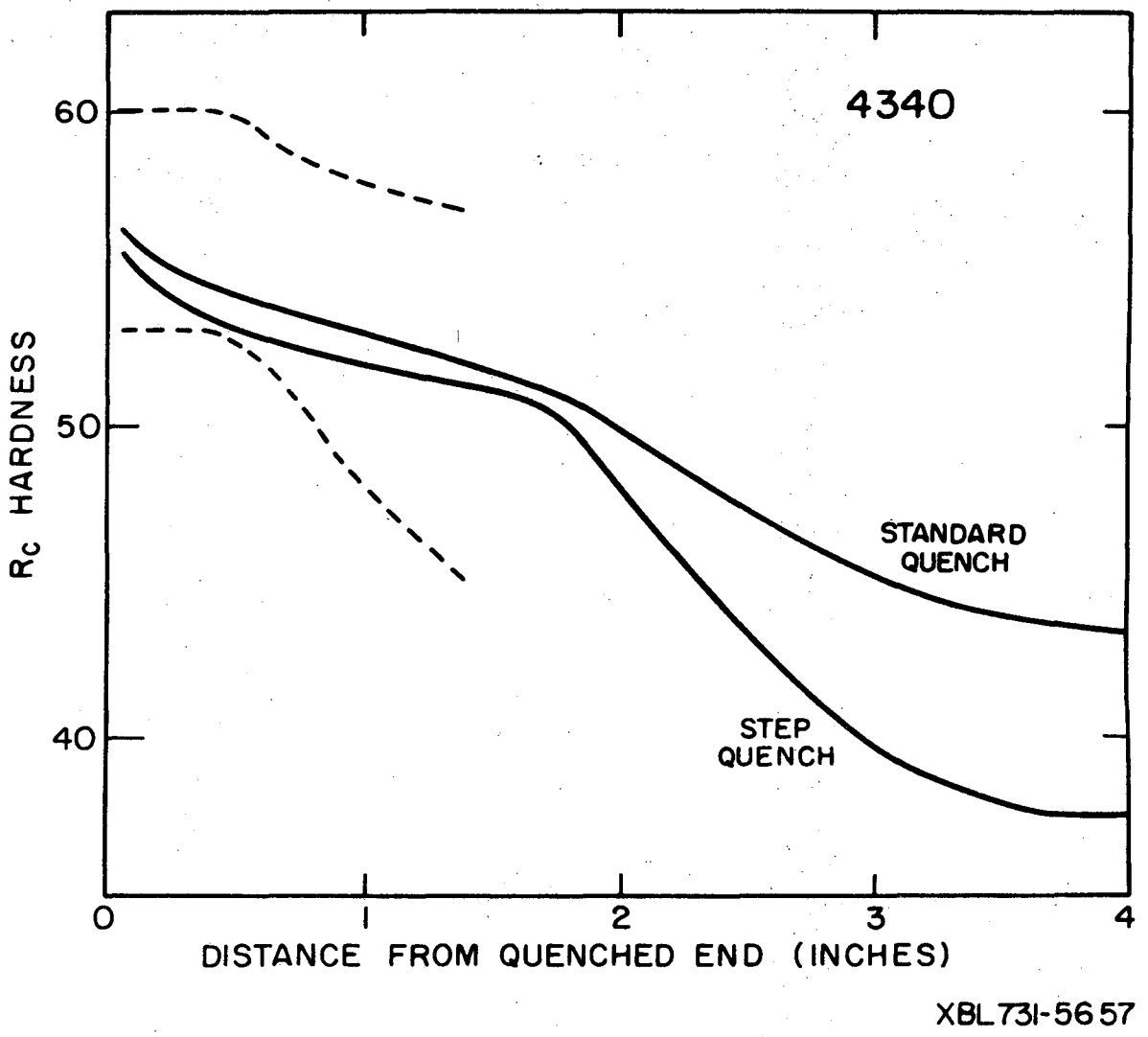

Fig. 10. The average hardenability curves for 4340 steel end quench specimens. The dotted lines represent published hardenability curve limits.[8]

contained inert argon atmospheres. The average hardenability curves for each of these heat treatments are shown in Figs. 9 and 10. There were no significant differences between the hardenability curves for the standard and step quenched specimens.

Next the end quench specimens were notched, cut, and ground to standard Charpy V-notch impact toughness bars[6] as shown in Fig. 5. During machining, the bars were sprayed with coolant to prevent heating.

For each alloy, the first test performed with the Charpy bars from the end quench specimens was the determination of a brittle transition curve for each Charpy bar position on the end quench specimen. In this series of tests, the Charpy bars were placed in an oil bath at the indicated temperature for 10 min., and then immediately broken at temperature.[6] The results of these tests are given in Table 2. The step quench heat treatment is shown to improve slightly the impact toughness properties of the 4340 steel and to degrade the impact toughness of the 4130 steel. These results did not correspond to the dramatic results obtained with K_{IC} fracture toughness specimens in Wood's[3] work. However, Wood also made some Charpy tests and found results similar to those reported here. Charpy impact toughness and K_{IC} fracture toughness tests do not always correlate well.

Tests were also made in which bars from each position on the end quench specimen were tempered before testing at room temperature. The Charpy bars in this series were placed in a temperature bath for 1 hr., removed to air cool, and impact tested. The tempering tests were performed only on the Charpy bars from end quench specimens given the

Table 2. Brittle Transition Curve Data Charpy V-notch Impact Toughness Values (Ft·lbs)

		4130 Testing Temperature				4340 Testing Temperature			
	Position	(RT) 70°F	(65.5°C) 150°F	(100°C) 212°F	(200°C) 392°F	(RT) 70°F	150°F	212°F	392°F
Standard Heat Treatment	1	10.6	23.7	17.5	20.5	4.2	5.2	5.0	16.0
	2	16.9	55.1	71.5	93.2	6.3	6.2	7.5	10.6
	3	17.9	-	78.5	95.0	6.2	5.7	7.0	9.4
	4	17.7	-	67.0	77.0	5.9	5.4	7.0	9.0
	5	14.5	42.0	57.5	65.0	5.4	6.2	6.4	12.5
	6	17.3	42.0	55.5	59.2	5.5	6.5	6.4	21.5
	7	19.3	39.2	57.1	61.5	5.6	6.4	8.0	21.0
	8	20.0	36.5	61.4	64.0	5.5	6.6	8.0	23.0
Step Quench Heat Treatment	1	10.0	15.0	12.0	14.0	5.0	6.8	8.0	13.5
	2	5.1	11.0	17.5	32.5	6.9	7.8	9.5	11.5
	3	6.6	17.0	21.0	50.0	6.0	7.2	8.5	10.5
	4	8.0	12.5	24.5	52.5	5.5	12.7	7.5	9.0
	5	8.0	11.2	31.5	55.5	6.9	8.8	10.0	12.5
	6	6.9	19.5	29.0	54.5	6.6	10.3	13.0	21.0
	7	7.7	13.2	30.0	54.5	9.1	7.4	11.0	27.5
	8	6.2	16.0	31.5	55.0	5.8	7.4	11.0	30.0

Charpy V-notch bars were held in temperature bath 10 minutes and then broken immediately at that temperature.

standard heat treatment; the results are given in Table 3. Auxiliary tests were performed to get a better idea of the toughness behavior. One of these was the heat treating of individual Charpy bars which were austenitized at the standard temperature for 30 min. and oil quenched. Two of these Charpy bars were tested as-quenched and the other two were tempered, air cooled, and then impact tested. These data are included in Table 3. In another series of tests, sets of Charpy bars from both alloys with the two austenitizing treatments were tempered at 392°F for 1 hr. and quickly tested at that temperature. The results are shown in Table 4. The longer tempering time had no significant affect on the Charpy values.

B. The Bundle Quench

In order to compare the toughness behavior of a quenched piece to that predicted by the end quench data, Charpy bars of each alloy were individually bound in the centers of bundles of steel blocks as shown in Fig. 7. To determine the cooling curves of the bundled Charpy bar quenched in agitated oil and agitated water, a 1/8 in. diameter hole was drilled through the bottom end to the center of the Charpy bar. A thermocouple, enclosed in a short length of 1/8 in. ceramic double hole tubing, was fitted into this hole and staked in by deforming metal at the hole opening over the end of the ceramic tubing. This held the thermocouple tip in firm contact with the metal at the center of the Charpy bar. The bundle was placed in a furnace at the standard austenitizing temperature and held there 1 hr.

Table 3. Charpy V-notch bars were tempered for 60 minutes in temperature bath, air cooled to room temperature and impact tested.

Tempering Data (ft·lbs)						
	4130 Tempering Temp.			4340 Tempering Temp.		
Position	A.Q	(302°F) 150°C	(392°F) 200°C	A.Q	150°C	200°C
1	10.6	20.3	17.0	4.2	6.5	11.0
2	16.9	19.8	28.0	6.3	9.6	8.0
3	17.9	25.3	34.3	6.2	7.8	7.5
4	17.7	22.6	35.7	5.9	7.1	6.0
5	14.5	21.5	20.1	5.4	6.8	6.0
6	17.3	19.5	22.9	5.5	6.2	6.0
7	19.3	20.7	25.0	5.6	7.5	7.5
8	20.0	20.3	24.0	5.5	7.5	7.5
Single bar, oil quenched	16.5		22.0	7.0		10.6

Table 4. Toughness Data for End Quench Charpys Tempered 60 Minutes and Broken at Temperature

Heat Treatment	Position on End Quench Specimen	Toughness Values (ft·lbs) 4130	4340
Standard	1	20.0	27.5
	2	86.5	14.0
	3	94.5	13.0
	4	83.0	11.5
	5	67.0	13.5
	6	62.0	13.5
	7	62.5	19.5
	8	65.0	20.0
Step Quenched	1	14.5	13.5
	2	37.0	12.5
	3	50.5	10.5
	4	57.5	9.0
	5	57.5	13.5
	6	54.0	23.0
	7	55.5	29.5
	8	55.0	34.5

The bundle was quenched vertically so that the thermocouple hole through the bottom of the Charpy bar contained a small gas pocket which prevented the quenching medium from reaching the thermocouple tip and affecting the recorded cooling curve. The cooling rates at 1300°F were determined from the cooling curves to be 59°F/sec for agitated water and 30°F/sec for agitated oil.

Three bundled bars of each alloy were water quenched and three more were oil quenched. The quenched bars were ground and notched to standard Charpy V-notch dimensions. Care was taken to notch the bars parallel to the rolling direction, as was done with the end quench specimen Charpy bars. One bar from each set was broken in the as-quenched condition, and the other two were tempered at the two temperatures used for tempering the end quench Charpy bars. In this way the toughness of the tempered bundle quenched bars could be compared with the toughness values of tempered end quench specimens. If it is true that the microstructures and properties can be predicted from the cooling rate at 1300°F in the end quench test, then the toughnesses of the bundle quenched Charpy bars should have been predictable, as illustrated in Fig. 11. The impact toughness values of the bundle quenched bars are compared with the values predicted by end quench toughness curves in Table 5 and Fig. 12. These results show the bundle quench values differ significantly from those predicted by the end quench curves. In fact, inverse correlation is indicated for the two steels. The Charpy values for the bundle quenched 4130 were lower than the values obtained from end quench test specimens,

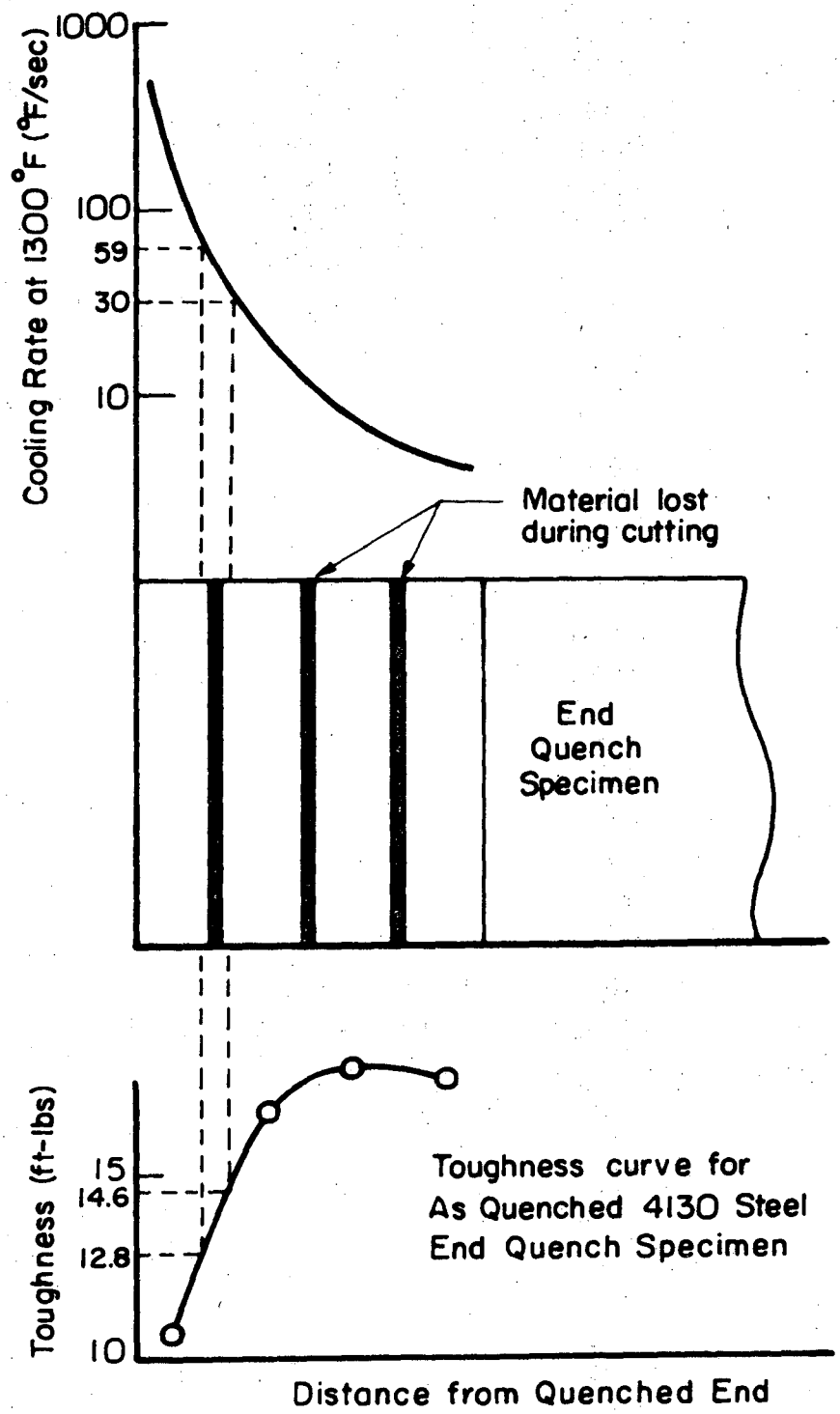

Fig. 11. Interpolation of an end quench toughness curve to obtain toughness values for the bundle quenched bars that would be predicted from their cooling rates at 1300°F.

Table 5. Comparison of Interpolated End Quench Toughness Values, Based on the Cooling Rate at 1300°F, and the Measured Bundle Quench Charpy Bar Toughness Values. (ft·lbs)

Tempering Temperature	4130 Alloy Water Bundle Quenched Value	4130 Alloy Predicted End Quench Value	4340 Alloy Water Bundle Quenched Value	4340 Alloy Predicted End Quench Value
As Quenched	9.0	12.8	6.2	5.2
302°F	14.2	20.1	16.4	8.0
392°F	15.1	22.3	23.4	9.4
	Oil Bundle Quenched Value	**Predicted End Quench Value**	**Water Bundle Quenched Value**	**Predicted End Quench Value**
As Quenched	8.5	14.6	13.9	5.9
302°F	17.1	20.0	13.9	9.0
392°F	18.4	25.8	12.5	8.5

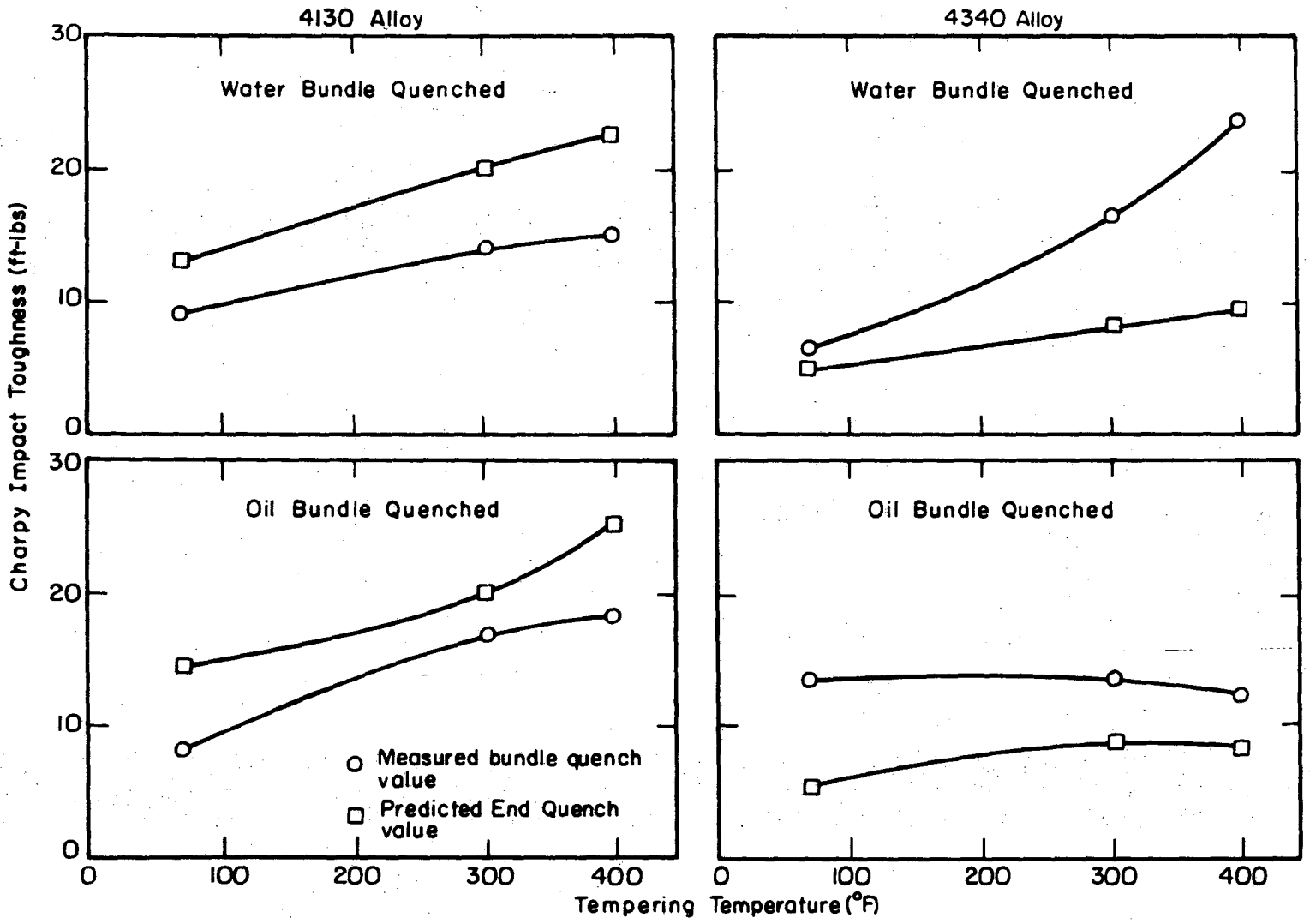

Fig. 12. Imapct toughness vs tempering temperature curves of the bundle quenched bars as compared to those predicted from interpolation of the end quench specimen toughness curves.

but the reverse was true for the 4340 steel.

After impact toughness testing, one of the fracture surfaces of the bundle quenched bars was sanded smooth and R_c hardness measurements were made at the center of each as-quenched specimen. These hardness values were compared with those predicted from the cooling rates and the hardenability curves (See Table 1 and Fig. 3 or 8). The bundle quench bar center hardness values and measured cooling rates are listed in Table 6 along with the hardness values predicted from the measured cooling rates at 1300°F along the end quench specimens. Also in Table 6, the measured cooling rates are compared to the cooling rates predicted from the measured hardness values. These results show that even though cooling rates at 1300°F may be identical in two pieces of the same steel quenched in different ways, the hardness values may not be the same. Conversely, identical hardness values in quench steel parts does not necessarily mean that the 1300°F cooling rates were the same.

C. The Bar Section Quench

The shape of the cooling curve of a quench piece is greatly affected by the geometry of the piece and the quenching conditions. It is not possible to predict the shape of the cooling curve on a continuous cooling transformation diagram from the cooling rate at 1300°F alone. To illustrate the extent to which the cooling curve is affected by the size, geometry and the quenching medium factors an experiment was performed in which round bar sections of various sizes were quenched in agitated water and in agitated oil.

Table 6. Comparison of Measured Bundle Quench Hardness Values and Cooling Rates at 1300°F to those Predicted from End Quench Hardenability Curves

Alloy	Quench	Measured Cooling Rate at 1300°F (°F/sec)	Measured R_c Hardness	R_c Hardness Values Predicted From Measured Cooling Rates	Cooling Rates at 1300°F Predicted From Measured Hardnesses (°F/Sec)
4130	Oil	30	38.0	33.5	44
4130	Water	59	46.0	38.6	125
4340	Oil	30	54.4	54.3	46
4340	Water	59	56.0	54.6	330

Thermocouples were placed at the bar centers and at the bar half radii (by the same method previously described in recording the cooling curves of the bundle quench specimens). From heat transfer considerations, any cylinder whose length is more than 5 times its radius is for all practical purposes an infinite cylinder.[7] Therefore, the bar sections 1, $1\frac{1}{2}$, 2, $2\frac{1}{2}$, and 3 inches in diameter had a length/radius ratios of 6 in order to negate the effect of heat flow through the ends during quenching. Some cooling rates at 1300°F for quenched bar sections are given in Fig. 13 (taken from Van Vlack[2]). The agitation of the quenching media was adjusted so that the results given in Fig. 13 were matched as closely as possible in this experiment. To represent the differences in the cooling curves, cooling rates were measured at 1300°F and 700°F. These cooling rates are given in Table 7 and are plotted in Fig. 14. The cooling rates at 1300°F and 700°F were also determined from the recorded cooling curves from the end quench specimens. These results are given in Table 8, and are also plotted in Fig. 14 which shows that it's possible with different sizes, geometries and quenching media, for two quenched pieces to have the same cooling rate at 1300°F but have vastly different cooling rates at 700°F (i.e. differently shaped cooling curves). Since the path of the cooling curve in the bainite and martensite regions of the continuous cooling transformation diagram (~ 700°F for 4130 and 4340 steels) would affect the final properties, differences in the toughness behavior of the bundle quenched bars and end quench specimens are to be expected. It is interesting to

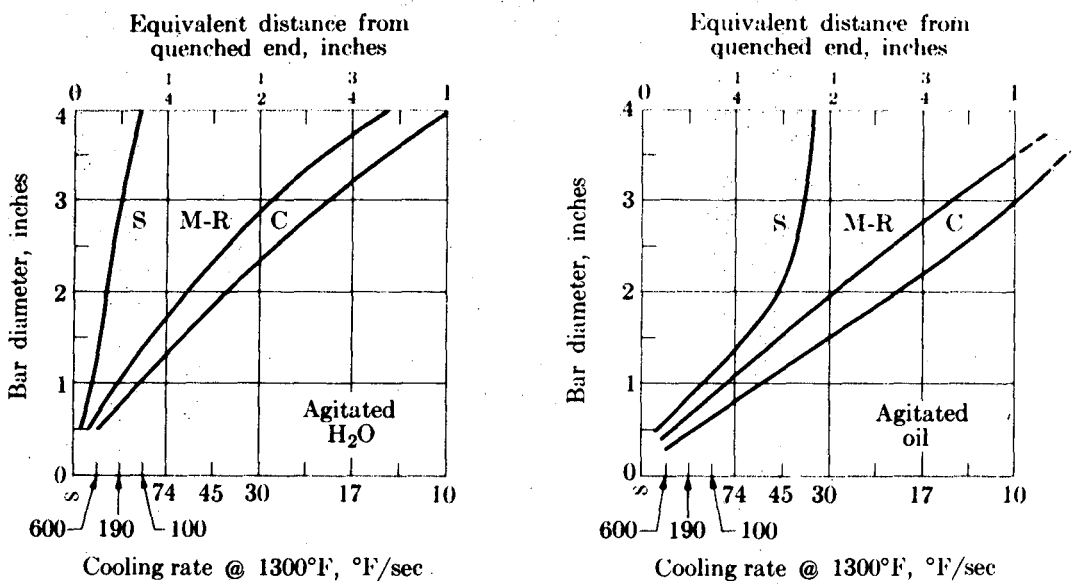

FIG. 11-31. Cooling rates in round steel bars quenched in (a) water, and (b) oil. Bottom abscissa, cooling rates at 1300°F; top abscissa, equivalent positions on an end-quenched test bar. (C, center; M-R, mid-radius; S, surface.)

XBL 735-582

Fig. 13. Bar section cooling rate curves (From Van Vlack[2])

Table 7. Bar Section Cooling Rate Data

Cooling Rates in Agitated Water

Bar Diameter (inches)	°F/Sec @ 1300°F Bar Center	°F/Sec @ 700°F Bar Center	°F/Sec @ 1300°F Half Radius	°F/Sec @ 700°F Half Radius
1	109	89	220	148
1 1/2	58	71	86	57
2	36	46	54	35
2 1/2	21	29	39	22
3	19	21	23	19

Cooling Rates in Agitated Oil

1	56	36	80	28
1 1/2	30	20	41	15
2	19	15	27	11.3
2 1/2	13	11.5	20	9.4
3	9	8.8	13	8.0

Table 8. Approximate Cooling Rates on the End Quench Specimen

Distance From Quenched End (inches)	°F/Sec @ 1300°F	°F/Sec @ 700°F
1/16	649	155
1/8	326	63
1/4	103	20
5/16	66	14.5
.45	37	9.5
.95	12	3.9
1.45	4.4	2.7
1.95	3.9	1.0

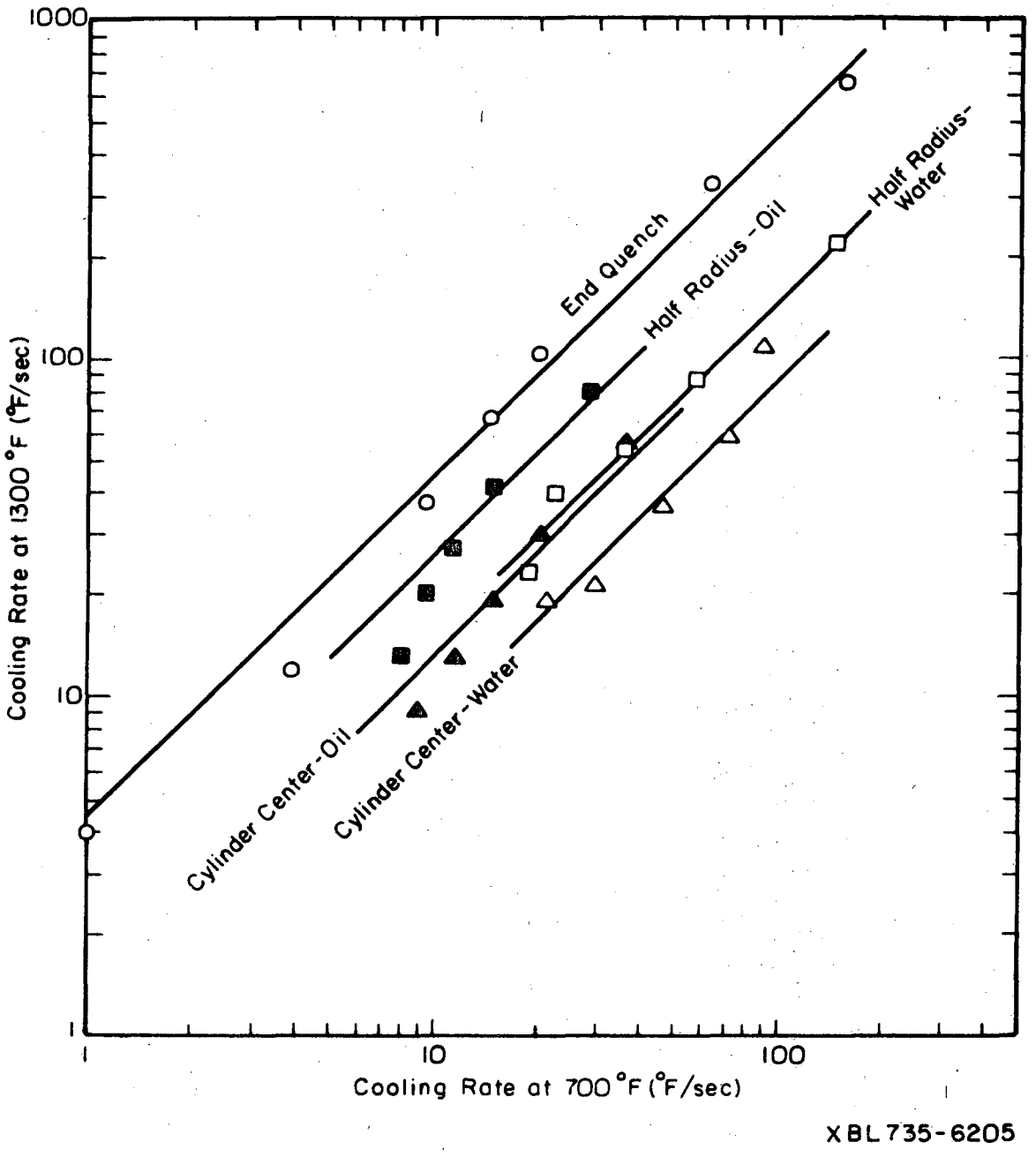

Fig. 14. Plots of the cooling rate at 1300°F vs the cooling rate at 700°F for various quench specimen sizes, geometries and quenching media.

note that a nearly linear relationship exists between the two cooling rates for a given geometry and quenching medium. (For further discussion of this relationship please see the appendix).

IV. DISCUSSION

The experimental results from this investigation show that accurate predictions of microstructure and properties of a quenched piece of steel cannot be made from end quench test results or ideal diameter correlations based on the cooling rate at 1300°F. Such predictions are not valid because they do not take into account the variability of the cooling curve shape at lower temperatures, caused by differences in specimen size, geometry and quenching medium.

Examination of the data given in Table 5 or Fig. 12 shows the toughness (as measured by the V-notch Charpy test) for a quenched piece predicted from end quench data is significantly inaccurate. The bundle quench toughness values for the 4130 alloy are consistantly below (as much as 42%) those predicted from the end quench data and the toughness values for the 4340 alloy are consistantly above (as much as 149%) those predicted from the end quench toughness curves. This means that microstructural differences, which may be difficult to detect optically, exist between the end quench specimen and the bundle quenched bar at points of equal cooling rate. The hardness-cooling rate comparisons of Table 6 show that the hardness values of the bundle quenched bars are not exactly the same as those of the end quench specimens for the same cooling rate at 1300°F, however, they correspond more closely than the comparisons of toughness behavior. This indicates that the property of hardness is not as sensitive to subtle microstructural changes as is the property of toughness. Then

different quenching conditions that correlate on the basis of equal hardness values at the quench piece centers can produce different microstructures and toughness properties.

These microstructural differences in pieces having the same cooling rate at 1300°F are understandable when one considers the variability in the paths a cooling curve can take from any given cooling rate at 1300°F. This idea is illustrated in Fig. 4 and the experimental results shown in Fig. 14 illustrate the extent to which the cooling curves vary with specimen size, geometry and quenching medium.

In conclusion, when using end quench data or ideal diameter--quench round plots such as those shown in Figs. 1, 2, and 3 it should be kept in mind that these correlations can not be relied upon to give an accurate prediction of the microstructure of the quenched piece in any given quenching situation. The end quench test is not useful as an accurate indicator of microstructure or mechanical properties.

ACKNOWLEDGEMENTS

The author extends his deepest appreciation to Professor Earl Parker for his guidance and creative discussion throughout this investigation.

Many thanks are due to Professor J. W. Morris, Jr. and Professor Frank Hauser for their review of this manuscript.

The assistance provided by the staff of the Inorganic Materials Research Division of the Lawrence Berkeley Laboratory is gratefully acknowledged. In particular, the author wishes to thank Walter Toutolmin (specimen processing), John Holthuis (technical advice), Sandy Stewart (materials acquisition), Alice Ramirez (manuscript preparation), and Gloria Pelatowski (line drawings).

This work was done under the auspices of the U.S. Atomic Energy Commission through the Inorganic Materials Research Division of the Lawrence Berkeley Laboratory.

APPENDIX

The Linear Relationship of the Cooling Rates

A nearly linear relationship exists between the two cooling rates, R_{1300} and R_{700}, for a given geometry and quenching medium as shown in Fig. 14. This relationship can be expressed in the form

$$R_{1300} = R_{700}\ (1+C)$$

where R_{1300} and R_{700} are the cooling rates at 1300°F and 700°F respectively and C is a constant that varies with specimen geometry, quenching medium, and location of the thermocouple. Values of C for the various conditions are:

Specimen	Quenching Medium	C
End Quench	Water Spray	3.55
Cylinder:		
Center	Water	-0.16
Center	Oil	0.35
Half Radius	Water	0.50
Half Radius	Oil	1.63

This is reseasonably valid for cooling rates above about 10°F/sec at 700°F, but at lower rates it yields calculated cooling rates at 700°F that are too low. This relationship suggests that it may be possible to determine, from known cooling rates at 1300°F, the cooling rates at some lower temperature for a series of geometrically similar

specimens of variable size once the C value has been determined.

The cooling curves, especially those taken at the cylinder centers, are affected by transformations moving from the surface of the specimen to the center during the quench. These transformations are of the form:

$$Fe_{\gamma} \rightarrow Fe_{\alpha} \qquad \Delta H_t = 215 \text{ cal/mole}^{1}$$

$$Fe_{\alpha_{paramagnetic}} \rightarrow Fe_{\alpha_{ferromagnetic}} \qquad \Delta H_t = 326 \text{ cal/mole}$$

These transformations occur nearly simultaneously in the 1040 steel used for the bar section quench experiment. (Using a value of 9.0 cal/°C/mole heat capacity, the heat liberated by these transformations would increase the temperature of the steel 60°C (140°F) if it were not lost to the quenching medium). These heats of transformations have the effect of hindering heat flow from the center of the quench piece until the whole piece has been transformed. The cooling rate at 1300°F at the center of the quench piece is decreased due to the heat of the transformations which causes a decrease in the thermal gradient near the center. (By the time the center of the piece has cooled to 1300°F the transformation fronts are very near arrival.) On the other hand the cooling rate at 700°F may be accelerated due to the steep thermal gradient left in the specimen after total transformation has been completed. For these reasons it is possible to have R_{700} greater than R_{1300} (i.e. a negative C value) as is the case for the centers of the water quenched cylinders. These explanations become evident when the cooling curves are examined.

REFERENCES

1. The Making, Shaping and Treating of Steel, United States Steel, Pittsburgh, 1971, Ninth edition. pp. 1097-1100, p. 292.
2. L. H. Van Vlack, Elements of Materials Science, Addison-Wesley Publishing Company, Inc. 1964, pp. 320-325.
3. W. E. Wood, Ph.D. thesis, Department of Materials Science and Engineering, University of California, Berkeley (1973).
4. R. D. Goolsby, (Ph.D. thesis) LBL-405 (1971).
5. "Standard Method of End-Quench Test for Hardenability of Steel," (ASTM Designation 255-67), 1971 Annual Book of ASTM Standards, American Society for Testing and Materials.
6. "Standard Methods for Notched Bar Impact Testing of Metallic Materials," (ASTM Designation E23-64), 1971 Annual Book of ASTM Standards, American Society for Testing and Materials.
7. J. B. Austin, The Flow of Heat in Metals, American Society for Metals, Cleveland, 1942, p. 104.
8. Metals Handbook, American Society for Metals, Vol. 1, 1961, Eighth edition. pp. 189-216.

TECHNICAL INFORMATION DIVISION
LAWRENCE BERKELEY LABORATORY
UNIVERSITY OF CALIFORNIA
BERKELEY, CALIFORNIA 94720